

# Direct measurements of the RHeq in salt mixtures including the contribution from metastable phases

I Rorig-Dalgaard (✉ [ird@byg.dtu.dk](mailto:ird@byg.dtu.dk))

Technical University of Denmark, Department of Civil Engineering

---

## Research article

**Keywords:** Equilibrium relative humidity, salt mixtures, dynamic vapor sorption instrument, metastable phases

**Posted Date:** January 19th, 2021

**DOI:** <https://doi.org/10.21203/rs.3.rs-147092/v1>

**License:**  This work is licensed under a Creative Commons Attribution 4.0 International License.

[Read Full License](#)

---

# Direct measurements of the $RH_{eq}$ in salt mixtures including the contribution from metastable phases

Inge Rörig-Dalgaard ([ird@byg.dtu.dk](mailto:ird@byg.dtu.dk))

Technical University of Denmark, Department of Civil Engineering, Kgs. Lyngby, Denmark

## Abstract

Accelerated salt-induced deterioration occurs by frequent changes across the equilibrium relative humidity ( $RH_{eq}$ ). Therefore, knowledge of the actual  $RH_{eq}$  of a salt mixture has a major impact on preventive conservation to ensure that the relative humidity (RH) does not cause a salt phase transition and in situ desalination as the dissolution of salt is the essential criterion to enable transport of salt (ions) in materials.

For decades, it has been possible to determine the  $RH_{eq}$  in salt mixtures with the user-friendly, thermodynamic-based ECOS-Runsalt software. However, the ECOS-Runsalt model is challenged by the influence of kinetics along with some limitations in regard to possible ion types and combinations.

A dynamic vapor sorption (DVS) instrument is used for the direct measurement of  $RH_{eq}$  and to deduce knowledge on the physicochemical nonequilibrium process related to the phase changes in salt mixtures. The experimentally measured  $RH_{eq}$  values in this study of NaCl-Na<sub>2</sub>SO<sub>4</sub>-NaNO<sub>3</sub>, NaNO<sub>3</sub>-Na<sub>2</sub>SO<sub>4</sub>, NaCl-NaNO<sub>3</sub>, NaCl-Na<sub>2</sub>SO<sub>4</sub>, and (NH<sub>4</sub>)<sub>2</sub>SO<sub>4</sub>-Na<sub>2</sub>SO<sub>4</sub> are in agreement with values from the literature. A comparison with thermodynamically calculated results makes it probable that the phase transition for some salts is significantly influenced by nonequilibrium conditions.

The present work bridges some of the existing gaps in regard to accuracy, including the effects of kinetics and the possible ions and combinations that may be found in situ. The proposed method makes it possible to determine a more representative  $RH_{eq}$  in relation to real conditions for the improved treatment of salt-infected constructs.

**Keywords:** Equilibrium relative humidity, salt mixtures, dynamic vapor sorption instrument, metastable phases.

## 1 Introduction

Natural changes in climatic conditions as a consequence of seasonal changes may promote the presence of salts, which can result in damaging salt phase changes [1]. Even timely limited climatic changes (a few hours) may result in salt phase transitions [2]. These salt phase changes may be avoided or reduced by preventive conservation, such as predicting the equilibrium relative humidity ( $RH_{eq}$ ) and following the establishment of favourable climatic conditions [1,3-5]. A few examples from praxis, where favourable climatic conditions have been established in the shape of climatic chambers to reduce salt-induced wall painting deterioration, can be observed in the Scrovegni Chapel in Padua, Italy and the Kirkerup, Magleby, Rørby and Sorø Monastery churches in Denmark.

In regard to in situ desalination campaigns, the supply of water has in many cases resulted in the redistribution of salt ions and their penetration to various depths, e.g., [6] is related to the fundamental limitation of this dissolution methodology [7], which prevented the desired desalination effect. Therefore, for desalination campaigns, knowledge of the  $RH_{eq}$  to ensure the dissolution of salts with the lowest possible water supply is desirable [8].

For single salts, the  $RH_{eq}$  is and has been well defined for decades [9]. An example of direct measurements of the  $RH_{eq}$  for a single salt is outlined in [10]. Here, the  $RH_{eq}$  of the single salt NaCl is determined with X-ray diffraction under controlled conditions of temperature and relative humidity (RH-XRD), and the disappearance of the respective educt phase peaks in the XRD patterns is used as criterion for the determination of  $RH_{eq}$  along with the reaction time until  $RH_{eq}$ .

Regarding salt mixtures, some  $RH_{eq}$  values are available in the literature, e.g., given in [11], and most two- and three-component salt mixtures can be thermodynamically calculated [11-16]. However, due to the current comprehensive possibilities, not all combinations are available in the

literature. Salt mixtures typically found in historic buildings are even more complex and are not limited to three-component salt mixtures [1], [17]. In the conservation science community, the thermodynamically based software ECOS-Runsalt [18-19] is becoming increasingly popular to predict the  $RH_{eq}$  of very complex salt mixtures based on measured ionic compositions (in mol or weight) from extracted samples. The ECOS-Runsalt software is very user friendly but is also known to have some limitations in regard to possible ion combinations since it relies on equilibrium conditions that do not include metastable phases. A previous contribution to the direct measurement of the  $RH_{eq}$  of single- and two-salt aerosol systems was in [11] and executed in a cell that could be evacuated and backfilled with water vapor; the phase transformation of the aerosol particle was monitored by laser light scattering. The RH at the transition point was determined by direct measurement of the water vapor pressure in the cell. In addition, they developed a theoretical model for the composition and temperature dependence. Another technique used to measure the  $RH_{eq}$  of salts is the use of a dynamic vapor sorption (DVS) instrument. In [20], it was made probable to determine the  $RH_{eq}$  of single salts with a DVS instrument by measuring mass changes during a constantly changing partial pressure across the point of zero mass changes that define  $RH_{eq}$ . To improve the accuracy of the  $RH_{eq}$  for single-salt results, a methodology was developed that took the properties of single salts into account [21]. This work was extended to include salt mixtures, and some preliminary examinations were reported in [22].

The present work makes use of the highly accurate calibration of the DVS instrument described in [21] to obtain a highly accurate and direct measurement of  $RH_{eq}$  for salt mixtures of NaCl, NaNO<sub>3</sub>, Na<sub>2</sub>SO<sub>4</sub> and (NH<sub>4</sub>)<sub>2</sub>SO<sub>4</sub> – Na<sub>2</sub>SO<sub>4</sub>. The determination of the  $RH_{eq}$  of salt mixtures of NaCl, NaNO<sub>3</sub>, and Na<sub>2</sub>SO<sub>4</sub> salts are chosen since these results can be compared with results from the literature [11-12], [15-16] just as results from the thermodynamically based ECOS-Runsalt program and the improved model presented in [23] based on an extended Pitzer formalism on the ion interaction for calculating water activity. The salt mixture (NH<sub>4</sub>)<sub>2</sub>SO<sub>4</sub> – Na<sub>2</sub>SO<sub>4</sub> is studied in the present work as an example of a salt that cannot be dealt with in the thermodynamically based ECOS-Runsalt software or in the improved model in [23] without updating the associated library, and comparisons are therefore only possible with experimental results [24]. These new measurement results, along with comparisons with previous experimental results and the results from the thermodynamically based ECOS-Runsalt software and improved model described in [23], form the basis for a discussion and assessment of the present suggested methodology for the direct measurement of the  $RH_{eq}$  in salt mixtures that includes the contribution of metastable phases.

## 2 Effect of additional salts on the $RH_{eq}$

### 2.1 Salt mixture behaviour on an aerosol scale

On an aerosol scale, the resulting dried particle is composed of a pure salt core with the least soluble salt surrounded by a mixed salt coating. The core composition is solely determined by the original aerosol composition, whereas the coating is identical to the eutonic composition and is independent of the original aerosol composition. If the ambient RH increases, the size of the dried particle remains unchanged until the RH in the atmosphere becomes identical to the eutonic water activity ( $a_w$ ). The solid coating with a eutonic composition at the particle surface is then dissolved in the absorbed water. Due to surface tension, the remaining pure salt solid core stays at the centre of the particle and is surrounded by a saturated solution of the eutonic composition. Further increasing the RH results in more water absorption by the particle, and part of the solid core of pure salt is dissolved to maintain water equilibrium between the solution and atmosphere. At a certain RH, which is a function of the overall composition of the original particle, the solid core of pure salt is completely dissolved into the solution, and the particle becomes a pure aqueous droplet [12].

### 2.2 Salt mixture behaviour linked to RH and gravimetric changes

In the case of at least two salts (3 different ion types), a multiphase region may exist during absorption. At the deliquescence point, mutual deliquescence relative humidity ( $RH_{Meq}$ ) is the RH at which the salt mixture starts to pick up moisture and thereby weight, and only one component in the solid mixture dissolves completely. Subsequently, the solution consists of an aqueous solution and undissolved solids following growth into a common saturated solution droplet at the second

critical RH ( $RH_{SCeq}$ ) at which the dissolution is completed with increasing water vapour condensation and thereby weight gain.

An increase in mass after the second critical RH is a consequence of continuous water droplet growth by water vapour condensation and is limited by the contact angle between the salt solution and substrate and may continue until a relatively high weight gain has been reached compared to the necessary weight gain to ensure dissolution of the salt. See Figure 1 for a visualized example of water absorption beyond the complete dissolution of salt.



Figure 1. Absorption of water molecules on 25 mg of NaCl(s) followed by vapor condensation in an aluminium pan ( $d = 6\text{ mm}$ ); a 453 % weight gain is observed. A weight gain of only 278 % is needed to ensure the complete dissolution of NaCl.

The mass increase, which is only related to water vapour condensation, differs in its mass increase function from the previous phase until  $RH_{SCeq}$  and may therefore be differentiated with another mass increase function. This observation allows for the separation of the abovementioned two phases based on the change in mass increase function at  $RH_{SCeq}$  with an increasing RH.

With a decreasing RH (desorption) from  $RH_{SCeq}$ , evaporation from the salt mixture solution occurs simultaneously with expulsion of water, resulting in one continuously decreasing mass function until  $RH_{Meq}$  is reached, which is where the salt mixture solution will crystallize. However, in [12], it is described that some salt mixtures are much less straightforward and termed nonideal. In such cases, with two salts (A and B) and a decreasing RH, one of the salts (A) eventually becomes saturated during one continuously decreasing mass function ( $f(x)_A$ ) and starts to form its crystalline phase. As the RH is further reduced, more of the solid phase of salt (A) forms at another decreasing mass function ( $f(x)_{A-B}$ ), and the residual solution becomes more concentrated in regard to salt (B). At a certain RH,  $RH_{Meq}$ , the two salts (A+B) crystallize together and form a mixed solid phase with a eutonic composition ( $RH_{Meq, (A+B)}$ ). The  $RH_{SCeq(A+B)}$  is always lower than the  $RH_{eq}$  of the individual solutes ( $RH_{eq, (A)}$  and  $RH_{eq, (B)}$ ).

In the following,  $RH_{eq}$  refers to  $RH_{SCeq}$  in the case of salt mixtures.

### 2.3 Calculation of the water activity in salt mixtures

The presence of additional ions impacts the solubility of each salt component. The equilibrium conditions, expressed as the water activity in salt mixtures ( $a_{w,mix}$ ), can be found by [24]:

$$\ln(a_{w,mix}) = X_1 \cdot Y_2 \cdot \ln(a_{w,12}) + X_3 \cdot Y_4 \cdot \ln(a_{w,34}) \quad (\text{I})$$

where  $X_1$  and  $X_3$  represent the cationic strength and  $Y_2$  and  $Y_4$  represent the anionic strength. The ionic strength (I) of each ion  $X_i$  and  $Y_i$  represent the cationic and anionic fractions for each component, respectively, that is:

$$X_1 = I_1 / (I_1 + I_3) \quad (\text{II})$$

$$X_3 = I_3 / (I_1 + I_3) \quad (\text{III})$$

$$Y_2 = I_2 / (I_2 + I_4) \quad (\text{IV})$$

$$Y_4 = I_4 / (I_2 + I_4) \quad (\text{V})$$

This effect is opposite to the common ion effect and is called the “secondary salt effect”. If additional ions are dissolved, the total ionic concentration of the solution increases, and interionic attractions become important. Water activities in salt mixtures will therefore be reduced compared to the stoichiometrically measured concentrations in solution including only the dissolution of one salt [25].

## 2.4 RH<sub>eq</sub> in praxis

In relation to the determination of the water activity in a solution by measurement, just as for many practical applications, the equilibrium conditions and ideal behaviour of water vapor may be assumed. The water activity may then be determined as [19]:

$$a_w = p_w/p_{w0}^0 = \frac{1}{100} \cdot RH \quad (VI)$$

where  $p_w$  and  $p_{w0}^0$  are the water vapor pressure above the solution and the saturation vapor pressure, respectively.

Therefore, to determine the water activity of an electrolyte solution, it is sufficient to directly measure the vapor pressure or the relative humidity above a solution of known composition at constant temperature because the water activity depends on the composition and concentration of the solution [4].

Based on examinations of the Na<sub>2</sub>SO<sub>4</sub> system, it is proposed that systems including hydrated states should incorporate additional phase equilibria that includes the hydration reaction with an equilibrium constant ( $K_{AB}$ ) as shown in [14]:

$$K_{AB} = 1/RH_{AB} \quad (VII)$$

where RH<sub>AB</sub> refers to the specific RH<sub>eq</sub> for the hydration-dehydration equilibrium. According to [4], most salts found in building materials form different hydrates.

## 3 The DVS instrument and determination of the RH<sub>eq</sub>

The introduction of a material sample into a sample chamber in a DVS instrument with connected software enables us to change and program the climatic conditions (temperature, air flow, continuously changing RH) surrounding the material sample and simultaneously monitor and record gravimetric changes (see Figure 2 for a schematic of the DVS instrument (DVS Advantage 1, Surface Measurements Systems, Alperton London, United Kingdom)).

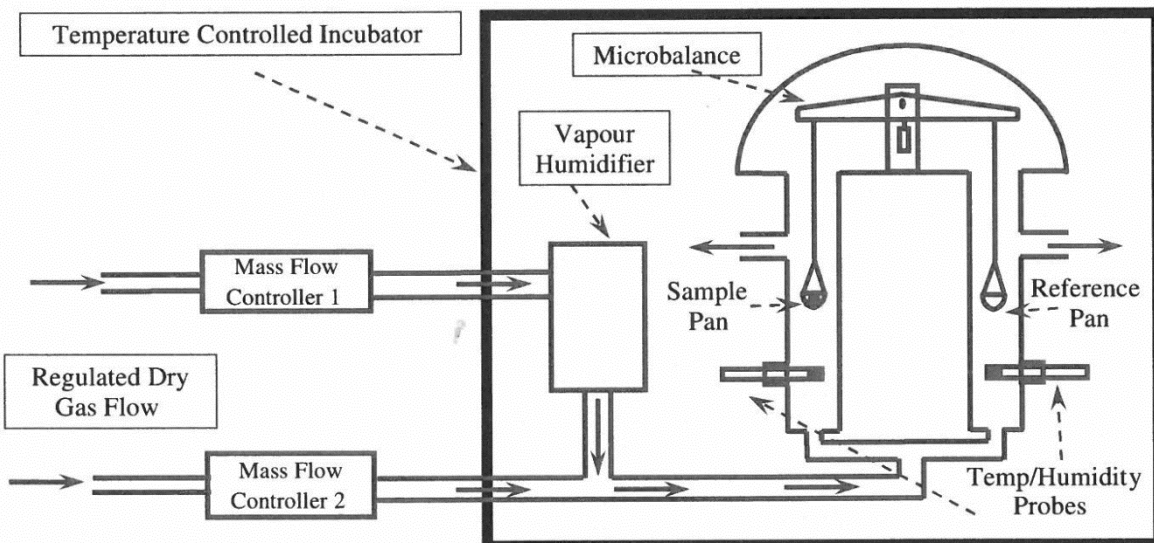


Figure 2. Schematic of the DVS instrument. Solid arrows show the direction of carrier gas flow. Reproduced with permission from [26].

The RH can be secured and measured with two independent systems: 1) a mixture of dry and moist air through valves based on prior calibration with single salts (termed open loop) and 2) a direct measurement with a dew point analyser within the sample chamber (termed closed loop). The accuracy of the open loop system is checked through calibration tests and performed with single salts covering RH values from 11 % to 93 % (LiCl; MgCl<sub>2</sub>; Mg(NO<sub>3</sub>)<sub>2</sub>; NaCl; KNO<sub>3</sub>). The salt

calibration principle is based upon the principle that the vapor pressure above a saturated salt solution is constant at a particular temperature (equation VI) and may reach equilibrium with its surroundings. For a more comprehensive description of the instrument, see [21].

When the actual RH approaches  $RH_{eq}$ , the total reaction time increases. When the total reaction time is high (shown for  $t > 2.5$  hours but dependent on salt type), the empirical kinetic equation can be linearized to interpolate the equilibrium conditions (where  $dm/dt = 0$ ) [21]:

$$\frac{dm}{dRH} = c(RH - RH_{eq}) \quad (\text{VIII})$$

where dm is the change in sample mass, dRH is the change in relative humidity and c is an experimentally determined constant.

Furthermore, since each salt differs in atomic composition, thereby resulting in different sizes, atomic structures, etc., each salt also differs in its properties, namely, their water absorption and desorption properties. Therefore, individual salt calibration tests were combined together with the specified salt preparation method in [21] to perform a highly accurate calibration. The salt calibration methods incorporate the following salt properties that influence calibration: the heat of solution, heat of condensation, and kinetics connected to the salt phase transition. These properties influence the microclimate surrounding the salts during calibration. In addition, both systems (open and closed) are used to ensure and measure the RH within the DVS, thereby supplementing each other and making the RH measurements as accurate as possible.

To achieve a highly accurate direct determination of the  $RH_{eq}$ , the measured values are adjusted with an experimentally determined difference between the measured values and the well-defined reference values [9] for single salts as described in [21].

## 4 Materials and Method

### 4.1 Preparation of salt mixtures

The approach was to use saturated salt solutions, i.e., the solution was saturated with respect to both or all three salts. This saturation was executed by adding the amount of salt corresponding to the solubility of each single salt at 100°C [27]. See Table 1 for the salts and amounts used for each salt mixture.

**Table 1:** Masses of each single salt added to 100 mL of distilled water for the preparation of the salt mixture.

	NaCl [g]	NaNO <sub>3</sub> [g]	Na <sub>2</sub> SO <sub>4</sub> [g]	(NH <sub>4</sub> ) <sub>2</sub> SO <sub>4</sub> [g]
NaCl-Na <sub>2</sub> SO <sub>4</sub> -NaNO <sub>3</sub>	39.1	180	42.7	
NaCl-NaNO <sub>3</sub>	39.1	180		
NaNO <sub>3</sub> -Na <sub>2</sub> SO <sub>4</sub>		180	42.7	
NaCl-Na <sub>2</sub> SO <sub>4</sub>	39.1		42.7	
(NH <sub>4</sub> ) <sub>2</sub> SO <sub>4</sub> -Na <sub>2</sub> SO <sub>4</sub>			42.7	103.8
(mass fraction Na <sub>2</sub> SO <sub>4</sub> 0.173)				

The salt mixtures were prepared by the addition of the salts into 100 mL of distilled water in a 1 L beaker. The beaker was placed in a pot with boiling water and covered with a slightly curved transparent watch glass on the top. The solution was heated until a temperature of approximately 100°C was obtained or until nucleation occurred at the surface of the solution, whereupon the beaker was removed from the pot. Next, a small amount of the hot solution was poured into a petri dish and placed in a fume hood to accelerate evaporation. Over time, crystals formed at the surface and gradually fell to the bottom of the beaker. After complete evaporation of the water, the salt crystals were collected.

## 4.2 Measuring methods

The measured  $\text{RH}_{\text{eq}}$  was influenced by kinetics and the initial state of the salt, and therefore, the measuring methodology influenced the result in terms of accuracy. The most influential measuring conditions in [21] were found to be the preconditioning of the salts. Preconditioning was related to the needed addition of water to the dry salt until  $\text{RH}_{\text{eq}}$  was obtained (see Table 2), and the reasoning was extensively described in [21]. The initial RH interval was centred around the  $\text{RH}_{\text{eq}}$  found in the literature as an initial approach for the measurement. In case a nonsatisfactory fit with equation VIII was found, an  $\text{RH}_{\text{eq}}$  was read out of the measuring data and subsequently became the centre of a new measuring interval. See Table 2 for the used salt preconditioning and measuring conditions.

Table 2. Overview of the salt preconditioning and measuring conditions.

	Added water	Interval	Measurement duration
	[%]	[% RH]	[hours]
NaCl-Na <sub>2</sub> SO <sub>4</sub> -NaNO <sub>3</sub>	24.4 +/- 3.1	+/- 5	11
NaCl-NaNO <sub>3</sub>	21.8 +/- 2.1	+/- 5	11
NaNO <sub>3</sub> -Na <sub>2</sub> SO <sub>4</sub>	27.5 +/- 2.3	+/- 5	11
NaCl-Na <sub>2</sub> SO <sub>4</sub>	25.1 +/- 6.6	+/- 5	11
(NH <sub>4</sub> ) <sub>2</sub> SO <sub>4</sub> -Na <sub>2</sub> SO <sub>4</sub> (mass fraction Na <sub>2</sub> SO <sub>4</sub> 0.173)	29.0 +/- 5.9	+/- 1.5	21

It should be noted that in most cases, the same measurement duration and RH interval were used. However, to obtain a satisfactory fit with the link described in equation VIII, it was necessary to adjust the measurement duration and size of the RH interval in relation to the salt mixture (NH<sub>4</sub>)<sub>2</sub>SO<sub>4</sub>-Na<sub>2</sub>SO<sub>4</sub>. Such adjustments of the measurement duration and RH interval have also been made, when relevant, in previous work [21].

## 5 Results and discussion

### 5.1 Check of the generated RH in the DVS instrument by single-salt calibration tests

Initial salt calibration tests on well-defined single salts are used to ensure the accuracy of the results for salt mixtures. Highly accurate salt calibration tests were carried out following the procedure described in [21]. Of special relevance are the salt calibration tests for the RH interval in which the salt mixtures are expected to have an  $\text{RH}_{\text{eq}}$  of 55-85 % RH. Therefore, calibration tests were carried out with single salts of Mg(NO<sub>3</sub>)<sub>2</sub> and NaCl (see Figure 3). The average measured difference from the reference value in [9] and the deviation in the identically performed experiment reveals a measuring inaccuracy between the experimentally determined values and the well-defined values in the literature. Since the single salts used for calibration purposes have well-defined  $\text{RH}_{\text{eq}}$  values and since the determined results in this study are found to have high accuracy, differences between the measured and reference results can be used to recalculate an accurate  $\text{RH}_{\text{eq}}$  ( $\text{RH}_{\text{eq},(\text{re-cal, DVS})}$ ) with the average measured difference. This approach is used in the following. A difference of 0.77 % RH and 0.72 % RH is found between the well-defined reference values from [9] and the determined  $\text{RH}_{\text{eq}}$  for Mg(NO<sub>3</sub>)<sub>2</sub> and NaCl in this study, respectively. Measured salt mixtures with an  $\text{RH}_{\text{eq}}$  of approximately 52 and 75 % RH are therefore recalculated to measure the deliquescence point with an added  $0.77 \pm 0.15$  % RH and  $0.72 \pm 0.12$  % RH, respectively ( $\text{RH}_{\text{eq,(\text{re-cal, DVS})}} = \text{RH}_{\text{measured with DVS}} + \text{RH}_{\text{diff, relevant RH}}$ ). It should be noted that the found  $\text{RH}_{\text{diff, relevant RH}}$  will differ in relation to the actual calibration of the DVS instrument.

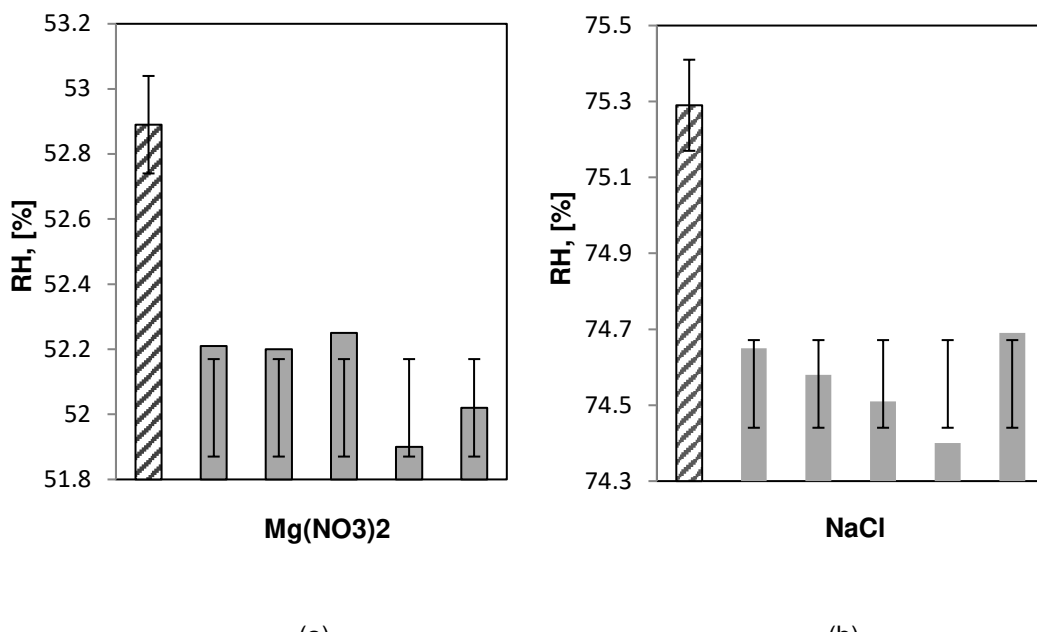


Figure 3. Reference RH<sub>eq</sub> from the literature [2] (shaded bars) together with experimentally obtained RH<sub>eq, DVS</sub> (solid bars), shown for a) Mg(NO<sub>3</sub>)<sub>2</sub> and (b) NaCl salts.

## 5.2 Determination of the RH<sub>eq</sub> in salt mixtures

The general definition of RH<sub>eq</sub> is the RH at which an absence of mass change exists, provided the temperature is constant. This criterion can and is also applied to salt mixtures.

The measured RH<sub>eq</sub> values for NaCl-Na<sub>2</sub>SO<sub>4</sub>-NaNO<sub>3</sub>, NaCl-NaNO<sub>3</sub>, NaNO<sub>3</sub>-Na<sub>2</sub>SO<sub>4</sub>, NaCl-Na<sub>2</sub>SO<sub>4</sub>; (NH<sub>4</sub>)<sub>2</sub>SO<sub>4</sub>-Na<sub>2</sub>SO<sub>4</sub> are shown in Table 3. Each measurement was performed in triplicate, thereby allowing the calculation of an average value and deviation. The reproducibility is high for all five salt mixtures and a standard deviation of +/-0.006-0.08 % RH is obtained (Table 3). This relatively low standard deviation is obtained by ensuring a constant mass change (dm) per change in RH (dRH), enabling the determination of the constant c in equation VIII, and minimizing the experimental error in the determined RH<sub>eq</sub>. Furthermore, the constant c enables an accurate determination of the intersection with the y-axis (see Figure 4), showing an absence of mass change at a specific RH, which is the definition of RH<sub>eq</sub>. An example of the measurement output data is shown in Figure 4. In Figure 5, the recalculated measured results are pictured together with results from the literature [11-12], [15-16], [24] and the ECOS-Runsalt calculated results [18-19] to obtain an overview and to clarify the differences and similarities among the various RH<sub>eq</sub> determination methods.

**Table 3:** Measured and re-calculated RH<sub>eq</sub> at 25°C. The re-calculated values are the average measured values +/- the measured difference from the reference values (shown in Figure 3).

Salt mixture	RH <sub>eq</sub> 1 <sup>st</sup> run	RH <sub>eq</sub> 2 <sup>nd</sup> run	RH <sub>eq</sub> 3 <sup>rd</sup> run	RH <sub>eq</sub> Average/d eviation	RH <sub>eq</sub> Re- calculated
NaCl-Na <sub>2</sub> SO <sub>4</sub> -NaNO <sub>3</sub>	65.96 ± 0.16	65.83 ± 0.03	65.89 ± 0.01	65.89 ± 0.08	66.61
NaCl-NaNO <sub>3</sub>	66.52 ± 0.01	66.19 ± 0.11	66.35 ± 0.14	66.35 ± 0.07	67.07
NaNO <sub>3</sub> -Na <sub>2</sub> SO <sub>4</sub>	72.48 ± 0.03	72.40 ± 0.01	72.53 ± 0.06	72.47 ± 0.03	73.19
NaCl-Na <sub>2</sub> SO <sub>4</sub>	73.78 ± 0.10	73.73 ± 0.08	73.50 ± 0.05	73.67 ± 0.03	74.39
(NH <sub>4</sub> ) <sub>2</sub> SO <sub>4</sub> -Na <sub>2</sub> SO <sub>4</sub> (mass fraction = 0.173 Na <sub>2</sub> SO <sub>4</sub> )	75.72 ± 0.07	75.32 ± 0.08	75.66 ± 0.07	75.57 ± 0.006	76.29

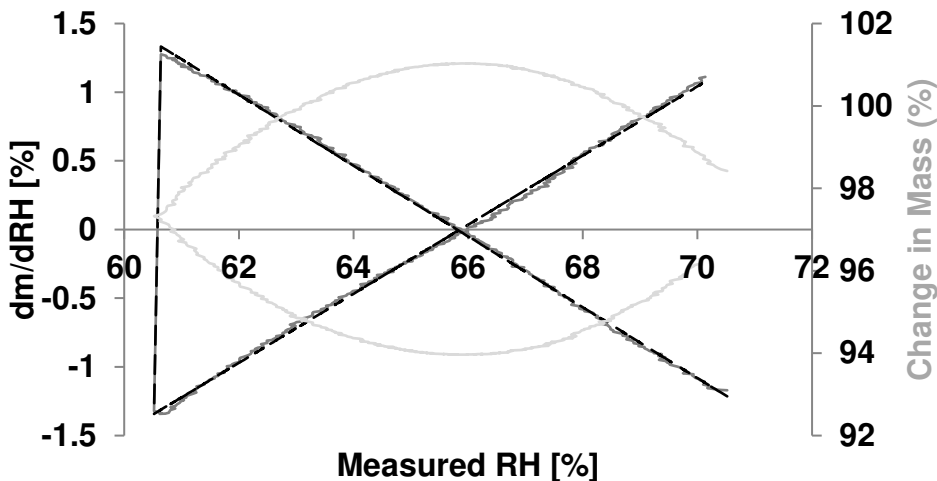


Figure 4. Example of the measurement results enabling the determination of the  $RH_{eq}$  of the salt mixture  $\text{NaCl-Na}_2\text{SO}_4\text{-NaNO}_3$  at  $25.0^\circ\text{C}$ . — (dark grey solid line) Measured  $dm/dRH$  with the dew point analyser within the sample chamber, — (black dotted line) fitted  $dm/dRH$ , — (bright grey solid line) change in mass in %.

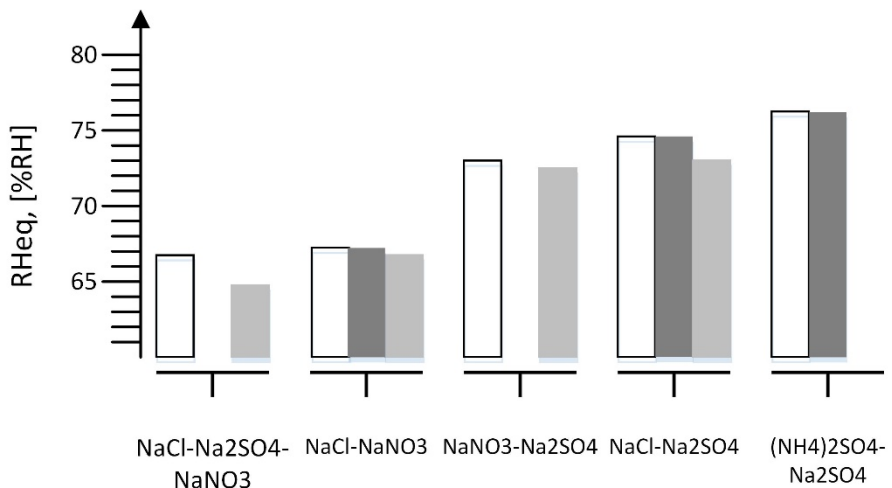


Figure 5.  $RH_{eq}$  of salt mixtures as obtained by different determination methods. □  $RH_{eq} (\text{re-cal, DVS})$  from Table 3 ■ Experimental data from the literature and ■ calculated results from the thermodynamically based ECOS-Runsalt model.

The recalculated  $RH_{eq(\text{re-cal DVS})}$  for  $\text{NaCl-Na}_2\text{SO}_4\text{-NaNO}_3$  (specifically,  $2/3\text{NaCl-3/10Na}_2\text{SO}_4\text{-21/10NaNO}_3$ ) was determined to be 66.61 % RH (see Table 3).

With a salt mixture consisting of the same salts, though differing in the number of moles where the amount of  $\text{NaNO}_3$  and  $\text{Na}_2\text{SO}_4$  corresponded to the solubility of each single salt at the eutonic composition, the  $RH_{eq}$  was determined to be  $71.8 \pm 0.5$  % RH in [11]. In [12], they characterized salt mixtures into two groups: simple and less simple systems. The former is independent of the mole fractions of the salts in this study, which is in contrast to the latter. Additionally, in [4], it is shown with examples that the solubility, saturation coefficients and crystallization properties of salt mixtures are strongly dependent on the mixture composition. Since the  $RH_{eq}$  in [11] is not comparable with the measured result in this study, it is not shown in Figure 5. However, the difference between  $RH_{eq(\text{re-cal DVS})}$  and [11] supports the effect of the specific number of moles on  $RH_{eq}$ .

With the present number of moles being 3.388, 0.6690, 0.3006 and 2.118 for sodium, chloride, sulfate and nitrate, respectively,  $RH_{eq(\text{ECOS-Runsalt})}$  was calculated to be 64.8 % RH. Figure 6 shows the calculated phases within the ECOS-Runsalt in the  $\text{NaCl-Na}_2\text{SO}_4\text{-NaNO}_3$  salt system within an RH interval ranging between 15 and 98 % darapskite ( $\text{NaNO}_3 \cdot \text{Na}_2\text{SO}_4 \cdot \text{H}_2\text{O}$ ), nitratine ( $\text{NaNO}_3$ ),

halite ( $\text{NaCl}$ ) and thenardite ( $\text{Na}_2\text{SO}_4$ ). As described in Section 2, at  $\text{RH}_{\text{Meq}}$ , only one component of the solid mixture dissolved completely and was thenardite; subsequently, the composition consisted of an aqueous solution and the undissolved solids of halite and nitratine. Following the production of a common saturated solution at the second critical RH ( $\text{RH}_{\text{SCeq}}$ ), dissolution was completed. Thus,  $\text{RH}_{\text{SCeq}}$  was calculated to occur at 64.8 % RH (see Figure 6). Following the approach in [14], it is proposed that systems that include the hydrated states should incorporate an additional phase equilibria part that includes the hydration reaction with an equilibrium constant of  $1/\text{RH}_{\text{AB}}$  (equation VII). Thus, in this salt mixture, a constant for the hydrated phase (caused by the presence of darapskite) was included,  $\text{RH}_{\text{eq}}(\text{ECOS-Runsalt including the hydrated phase}) = \text{RH}_{\text{eq}}(\text{ECOS-Runsalt}) + 1/\text{RH}_{\text{eq}}(\text{ECOS-Runsalt, NaCl-Na}_2\text{SO}_4) = 64.8\% + 1/0.648 = 66.34\% \sim \text{RH}_{\text{eq}}(\text{re-cal DVS})$ .

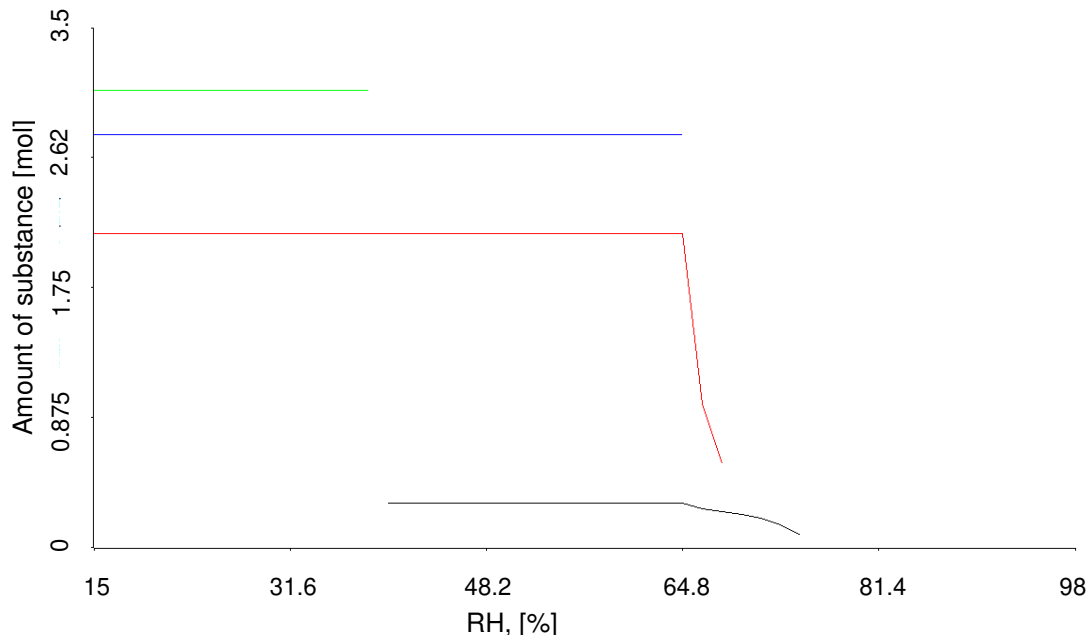


Figure 6. ECOS-Runsalt output diagram for the salt mixture  $\text{NaCl-Na}_2\text{SO}_4\text{-NaNO}_3$  with the number of moles being 3.4, 0.7, 0.3 and 2.1 for sodium, chloride, sulfate and nitrate, respectively, at 25°C. The  $\text{RH}_{\text{eq}}(\text{ECOS-Runsalt})$  was calculated to be 64.8 %. Black indicates the content of darapskite ( $\text{NaNO}_3\text{Na}_2\text{SO}_4\cdot\text{H}_2\text{O}$ ), red indicates nitratine ( $\text{NaNO}_3$ ), blue indicates halite ( $\text{NaCl}$ ) and green indicates thenardite ( $\text{Na}_2\text{SO}_4$ ).

$\text{RH}_{\text{eq}}(\text{re-cal DVS})$  for  $\text{NaCl-NaNO}_3$  (specifically  $2/3\text{NaCl-}3/10\text{Na}_2\text{SO}_4$ ) was determined to be 67.07 % RH (see Table 3). In [12], the  $\text{RH}_{\text{eq}}$  for this salt mixture was thermodynamically calculated to be 67 % RH. In [11], the  $\text{RH}_{\text{eq}}$  of the  $\text{NaCl-NaNO}_3$  salt mixture at a eutonic composition, where the composition of both salts reached their solubility limit in the solution, was measured to be  $68.0 \pm 0.4$  % RH. In [15], the deliquescence point was calculated for various aqueous solutions of  $\text{NaCl-NaNO}_3$  salts. Since the above salt mixture was an aqueous solution, the results were non-comparable; however, it is noticed that the water activity was relatively strongly influenced by the molar ratio, which may also be the reason for the slightly deviating results between  $\text{RH}_{\text{eq}}(\text{re-cal DVS})$  and [12]. With the present number of moles being 2.787, 0.6690 and 2.118 for sodium, chloride and nitrate, respectively, the  $\text{RH}_{\text{eq}}(\text{ECOS-Runsalt})$  was calculated to be 66.46 % RH. According to the ECOS-Runsalt results, only halite and nitratine were present in the salt mixture; additionally, no salt hydrates formed. With the improved thermodynamically based model described in [23], the  $\text{RH}_{\text{eq}}$  was calculated to be 66.76 % (by the corresponding author of [23]). In short,  $\text{RH}_{\text{eq}}(\text{ECOS-Runsalt}) < \text{RH}_{\text{eq, litt [23]}} < \text{RH}_{\text{eq}}(\text{re-cal DVS}) = \text{RH}_{\text{eq, litt [3]}}$  (see Figure 5).

The  $\text{RH}_{\text{eq}}(\text{re-cal DVS})$  was determined to be 73.19 % RH for  $\text{NaNO}_3\text{-Na}_2\text{SO}_4$  (see Table 3). In [11], the  $\text{RH}_{\text{eq}}$  for  $\text{NaNO}_3\text{-Na}_2\text{SO}_4$  was found to be  $72.2 \pm 0.2$  %, where the number of moles of  $\text{NaNO}_3$  and  $\text{Na}_2\text{SO}_4$  corresponded to the solubility of each single salt at the eutonic composition. Therefore, the number of moles of the above salts were not identical between the present work and [11]. In [15], it was shown that for this specific salt mixture,  $\text{RH}_{\text{eq}}$  was a function of the total molality of

$\text{NaNO}_3$  and  $\text{Na}_2\text{SO}_4$  similar to the ratio between  $\text{NO}_3^-$  and  $\text{SO}_4^{2-}$  significantly affecting the  $\text{RH}_{\text{eq}}$ ; thus, the  $\text{RH}_{\text{eq}}$  in total may vary between 55 and 85 % RH. In the present work  $x_{\text{NO}_3}$  equalled 0.876. In [16], the  $\text{RH}_{\text{SCEq}}$  was calculated under similar (but not identical) conditions, providing  $x_{\text{NO}_3} = 0.9$  at 23.5°C and read to 73.8 % RH in the graph. Applying ECOS-Runsalt and the present number of moles of 2.719, 2.118 and 0.3006 for sodium, nitrate and sulfate, respectively,  $\text{RH}_{\text{eq}}(\text{ECOS-Runsalt})$  was calculated to be 72.58 % RH. The calculated salt conditions were for darapskite, nitratine and thenardite. Taking the hydration constant into account as proposed in [14], as a consequence of the presence of darapskite,  $\text{RH}_{\text{eq}}(\text{ECOS-Runsalt including the hydrated phase}) = \text{RH}_{\text{eq}}(\text{ECOS-Runsalt}) + 1/\text{RH}_{\text{eq}}(\text{ECOS-Runsalt, NaNO}_3\text{-Na}_2\text{SO}_4) = 72.58 \% + 1/0.7258 = 73.96 \%$ . However, it may be considered that the hydration constant should be related to the concentration of the solution, as this would influence the chemical potential, which again would influence the activity,  $a_w$ , as stated in [4]. In [15], aqueous solutions of the salt  $\text{NaNO}_3\text{-Na}_2\text{SO}_4$  showed that the water activity was strongly influenced by the molar ratio. With the more advanced thermodynamically based model described in [23], the  $\text{RH}_{\text{eq}}$  was calculated to be 73.52 % (by the corresponding author of [23]); notably, taking into account the presence of darapskite, the relations become further complicated, and with a surplus of  $\text{NaNO}_3$ , as in this case, a mixture consisting solely of nitratine and darapskite would come into existence [16].

The re-calculated  $\text{RH}_{\text{eq}}$  ( $\text{RH}_{\text{eq (re-cal DVS)}}$ ) for  $\text{NaCl-Na}_2\text{SO}_4$  (specifically 2/3 $\text{NaCl}$ -3/10 $\text{Na}_2\text{SO}_4$ ) was determined to be 74.39 % RH (see Table 3). This result was consistent with and did not significantly differ from the  $\text{RH}_{\text{eq}}$  found by [11],  $74.2 \pm 0.3$  % RH ( $\text{RH}_{\text{eq(litt[11])}}$ ). In [15], aqueous solutions of  $\text{NaCl-Na}_2\text{SO}_4$  salts and their water activity were found to be relatively limited due to the molar ratios of  $\text{Cl}^-$  and  $\text{SO}_4^{2-}$ .

With the present number of moles of 1.270, 0.6690 and 0.3006 for sodium, chloride and sulfate, respectively, the  $\text{RH}_{\text{eq}}(\text{ECOS-Runsalt})$  was calculated to be 73.1 %. Notably,  $\text{RH}_{\text{eq (re-cal DVS)}} \sim \text{RH}_{\text{eq(litt[11])}} > \text{RH}_{\text{eq}}(\text{ECOS-Runsalt})$ , where  $\text{RH}_{\text{eq}}(\text{ECOS-Runsalt})$  deviates by 1.3-1.1 % RH from  $\text{RH}_{\text{eq (re-cal DVS)}}$  and  $\text{RH}_{\text{eq(litt)}}$  (see Figure 5 for an overview). According to the ECOS-Runsalt model, mirabilite ( $\text{Na}_2\text{SO}_4\cdot 10\text{H}_2\text{O}$ ), thenardite and halite are formed in a salt mixture. Following the approach in [14], an additional phase equilibria constant was included due to the formation of the hydrated phase mirabilite. Therefore,  $\text{RH}_{\text{eq}}(\text{ECOS-Runsalt including the hydrated phase}) = \text{RH}_{\text{eq}}(\text{ECOS-Runsalt}) + 1/\text{RH}_{\text{eq}}(\text{ECOS-Runsalt, NaCl-Na}_2\text{SO}_4) = 73.1 \% + 1/0.731 = 74.47 \%$ . With the improved thermodynamically based model described in [23], the  $\text{RH}_{\text{eq}}$  was calculated to be 74.33 % (by the corresponding author of [23]), and when including the hydrated state,  $\text{RH}_{\text{eq}}(\text{ECOS-Runsalt including the hydrated phase}) \sim \text{RH}_{\text{eq (re-cal DVS)}} \sim \text{RH}_{\text{eq(litt[11])}} \sim \text{RH}_{\text{eq(litt[23])}}$ . Furthermore, the results for  $\text{RH}_{\text{eq(re-cal DVS), NaCl-Na}_2\text{SO}_4}$  and  $\text{RH}_{\text{eq(re-cal DVS), NaCl}}$  clarified that it was possible to measure a significant difference in the  $\text{RH}_{\text{eq}}$  between  $\text{NaCl}$  ( $75.29 \pm 0.12$  % RH) and  $\text{NaCl-Na}_2\text{SO}_4$  ( $74.2 \pm 0.3$  % RH), with two salts having an  $\text{RH}_{\text{eq}}$  relatively close to each other. This possible differentiation between salts with  $\text{RH}_{\text{eq}}$  values relatively close to each other was made possible by the high reproducibility of the  $\text{RH}_{\text{eq(re-cal DVS)}}$  results that had an accuracy of 0.12 % RH (see Figure 3).

The  $\text{RH}_{\text{eq(re-cal DVS)}}$  for  $(\text{NH}_4)_2\text{SO}_4\text{-Na}_2\text{SO}_4$  (mass fraction of 0.173 in regard to  $\text{Na}_2\text{SO}_4$ ) was determined to be 76.29 % RH. In [20], the  $\text{RH}_{\text{eq}}$  for the  $(\text{NH}_4)_2\text{SO}_4\text{-Na}_2\text{SO}_4\text{-H}_2\text{O}$  system was described as being dependent on the actual ion fractions (equation I) and non-ideal behaviour. With a mass fraction of 0.171 % with respect to  $\text{Na}_2\text{SO}_4$ , the  $\text{RH}_{\text{eq}}$  was estimated to be between 75.20 and 76.20 % RH based on electro-dynamic particle balance measurements of the water activities of highly concentrated solutions and from the phase diagram in [24]. This result was in agreement with the  $\text{RH}_{\text{eq (re-cal DVS)}}$  of 76.29 % RH with a similar mass fraction of 0.173 in regard to  $\text{Na}_2\text{SO}_4$ . These results cannot be compared with the calculated  $\text{RH}_{\text{eq}}$  from the ECOS-Runsalt software, as this ion-type  $\text{NH}_4$  is not included [21] or used as a default in the improved model in [23]. ECOS-Runsalt was developed using the molality-based thermodynamic approach of Pitzer [18-19] and calculates in regard to mole fractions; thus, ECOS-Runsalt is restricted to the mole fractions of salts that are most commonly encountered in conservation:  $\text{Na}^+$ ,  $\text{K}^+$ ,  $\text{Mg}^{2+}$ ,  $\text{Ca}^{2+}$ ,  $\text{Cl}^-$ ,  $\text{NO}_3^-$ ,  $\text{SO}_4^{2-}$  and  $\text{H}_2\text{O}$  and excludes mixtures containing both  $\text{Ca}^{2+}$  and  $\text{SO}_4^{2-}$ . Notably, model parameters are provided and validated for the  $\text{Na}^+ - \text{K}^+ - \text{Cl}^- - \text{NO}_3^- - \text{SO}_4^{2-} - \text{H}_2\text{O}$  system in the improved model in [23]. In [28],  $\text{NH}_4^+$  is considered a traditional ion in regard to historical constructions, and as such, it is advised to be determined as a default. The need to exclude mixtures containing both  $\text{Ca}^{2+}$  and  $\text{SO}_4^{2-}$  in ECOS-Runsalt is related to practical limitations, as one frequently comes across this combination in praxis. However, this and other limitations are reported to be caused by the fact

that it was not possible to refine the system to the extent that had originally been envisaged within the project period [21].

Having shown consistency among the measured experimental data in this study by use of the DVS instrument, measurements and calculations from the literature and thermodynamic calculated values from the ECOS-Runsalt model and improved model in [23] for a mixture consisting of up to three salts, the determined  $RH_{eq}$  with the DVS instrument seemed to be generally valid. According to [18-19], data for quaternary (four ions) or higher mixtures are not required for the parameterization of the model, as experience has shown that the modelling of the thermodynamic properties of multicomponent electrolyte mixtures only requires two or three particle interactions.

### 5.3 Hypothesis for the determined difference in $RH_{eq}$ between ECOS-Runsalt and the DVS instrument

All the present determined  $RH_{eq}$  (re-cal DVS) pictured in Figure 5 did not differ significantly from the comparable results in the literature and were in good agreement with those results obtained with the more advanced thermodynamically based model described in [23]. However, comparing the results with the results obtained with the thermodynamically based software ECOS-Runsalt, there were differences (minimal to significant).

In ECOS-Runsalt, it is assumed that the entire salt system is in equilibrium with its surroundings at all times [18-19] and therefore does not include the effect of kinetics. However, for some salt mixtures, the kinetics significantly influence the growth of crystals. The kinetics are primarily influenced by the difference between the ambient conditions and equilibrium conditions ( $RH_{actual} - RH_{eq}$ ); however, for some salts, the temperature is also of major importance. A visual example of the kinetics influence on deliquesce is shown in Figure 7.

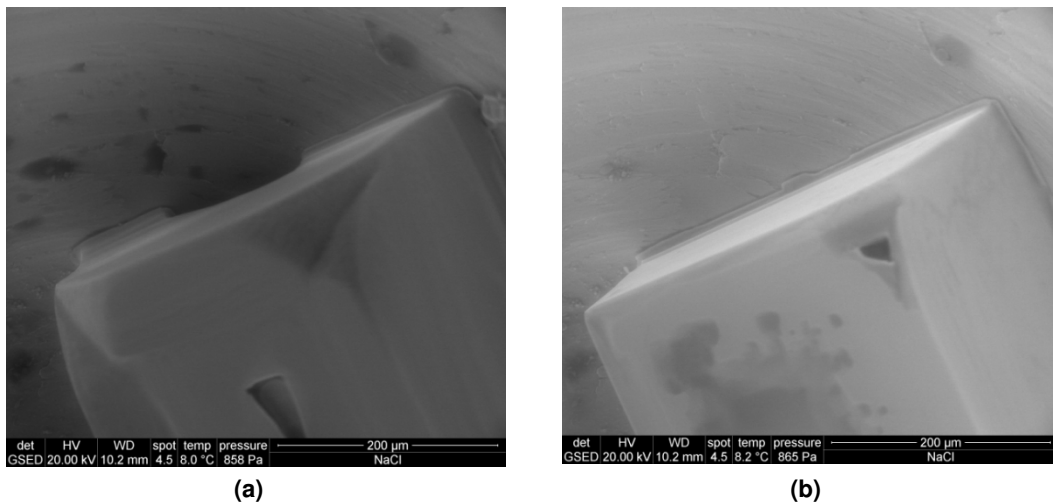


Figure 7. Visualization of the kinetic influence ( $\Delta RH$ ) on a salt (NaCl) phase transition studied by the application of a cooling stage in an ESEM: a) reference equilibrium conditions and b) influence of a change of 0.1 % RH for 19 hours [29].

The existence of metastable phases as a consequence of nonequilibrium conditions also influences salt formation. For example, the phase diagram for the binary system of  $Na_2SO_4-H_2O$  is significantly more complex than originally predicted. Experimental investigations can document the existence of two metastable phases, which are caused by the influence of kinetics. In equilibrium models, metastable phases are not predicted. However, in [14], metastable equilibrium is incorporated in the thermodynamic models to simulate the existence of metastable phases, which is a necessary part of the  $Na_2SO_4 - H_2O$  system, thereby obtaining a full picture for understanding deterioration mechanisms. The phase diagram pictures both stable and metastable phases illustrating that the metastable phases have both higher and lower  $RH_{eq}$  than the stable phases depending on the temperature. This result is a consequence of the precipitation sequence that is under kinetic control. The crystallization of the anhydrous phases proceeds at higher rates than the

precipitation of the hydrates. Therefore, the formation of the anhydrous phase is particularly favoured at low relative humidity [14]. Since the contribution from metastable phases is not included in the thermodynamically based ECOS-Runsalt model [18-19], the presence of metastable phases will result in deviating results for the  $RH_{eq}$  (ECOS-Runsalt).

When comparing  $RH_{eq}$  (re-cal DVS) with  $RH_{eq}$  (ECOS-Runsalt), the results with the highest deviation are salt mixtures including hydrated salts, with deviations of 1.8 % RH and 1.3 % RH for NaCl-Na<sub>2</sub>SO<sub>4</sub>-NaNO<sub>3</sub> and NaCl-Na<sub>2</sub>SO<sub>4</sub>, respectively. For NaCl-Na<sub>2</sub>SO<sub>4</sub>-NaNO<sub>3</sub> and NaCl-Na<sub>2</sub>SO<sub>4</sub> salts, the deviation could fully be accounted for by following the approach in [14] to include a hydration constant. The salt mixture NaNO<sub>3</sub>-Na<sub>2</sub>SO<sub>4</sub> also formed a hydrated salt (darapskite), where inclusion of the hydration constant resulted in  $RH_{eq}$  (re-cal DVS) <  $RH_{eq}$  (ECOS-Runsalt including the hydrated phase) by 0.8 % RH. In the case of NaCl-NaNO<sub>3</sub>, ECOS-Runsalt did not predict the formation of hydrated salts, and a hydration constant was therefore not included; thus it was seen that  $RH_{eq}$  (re-cal DVS) >  $RH_{eq}$  (ECOS-Runsalt) by 0.6 % RH.

The ECOS-Runsalt model was validated with water activity measurements. Direct vapor pressure measurements were obtained above single-salt solutions (a deviation of approximately 0.2 %). Attempts were also made to use standard RH and T sensors for the measurements of water activities with a sensor. A Testo 601 instrument (Testotherm) was used to test solutions of LiCl and NaCl and standard solutions of known water activity. The deviations for these measurements were approximately 3-4 % RH, and the authors described that such a deviation was insufficient to obtain water activities or osmotic coefficients with the accuracy required for the determination of binary model parameters. However, they reported that this type of measurement was much less time consuming than direct measurements and might be helpful for model validation [18-19].

Therefore, it may be argued that the reason for the ECOS-Runsalt calculation of  $RH_{eq}$  deviating from  $RH_{eq}$  measured with the DVS instrument and the experimental results from the literature is caused by the following: 1) equilibrium conditions are assumed at all times and do not include hydration reactions and 2) the precision of the validation data. The above assumptions are further supported by the fact that the improved thermodynamically based model described in [23] provides results that differ by only +/- 0.33 % RH from the measured  $RH_{eq}$  (re-cal DVS) for three out of the five salt mixtures in this study; thus, it is possible to calculate with the proposed model.

## 6 Conclusion

The present work contributes to enabling a more accurate determination of  $RH_{eq}$  in salt mixtures, thereby preventing or minimizing accelerated salt-induced deterioration. This determination is through the direct measurement of  $RH_{eq}$  in salt mixtures utilizing a DVS instrument. As a consequence of using a previously developed methodology for a highly accurate calibration of the equipment, it is possible to determine  $RH_{eq}$  with a similarly high accuracy (< 0.2 % RH).

The direct measurements of  $RH_{eq}$  take into account the fractioning of salts in mixtures, which has been recently reported to influence  $RH_{eq}$  due to metastable phases.

There was consistency among the measured experimental data in this study with the DVS instrument, experimentally measured data and thermodynamically based calculations from the literature, and thermodynamically calculated values by the ECOS-Runsalt model and an improved thermodynamically based model for a mixture consisting of two or three salts. This consistency was found for all five salt mixtures that were studied (NaCl-Na<sub>2</sub>SO<sub>4</sub>-NaNO<sub>3</sub>, NaCl-NaNO<sub>3</sub>, NaNO<sub>3</sub>-Na<sub>2</sub>SO<sub>4</sub>, NaCl-Na<sub>2</sub>SO<sub>4</sub>, (NH<sub>4</sub>)<sub>2</sub>SO<sub>4</sub>-Na<sub>2</sub>SO<sub>4</sub>), and the use of the DVS instrument for the determination of  $RH_{eq}$  seemed to be generally valid. This result makes it possible to directly measure the  $RH_{eq}$  in salt mixtures with an arbitrary number of ion types, which would occur in real-world, in situ applications. Therefore, the proposed methodology could be the advancement needed for the accurate determination of  $RH_{eq}$  and for subsequent decisions on favourable climatic conditions to avoid or reduce phase transitions without restricting validity to specific ion types and combinations.

Through the proposed direct measurements of  $RH_{eq}$  of salt mixtures forming hydrates, it was identified that the use of the thermodynamically based ECOS Runsalt software in some cases

resulted in significantly different  $RH_{eq}$  values. This observation was found when comparing the experimentally determined  $RH_{eq}$  in this work with the experimentally determined results from previous research and with the improved thermodynamically based model described in [23]. This result may be explained by the fact that in the ECOS-Runsalt model, equilibrium conditions were assumed at all times and did not include the contribution of metastable phases together with the precision of the validation data. Additionally, some ions (e.g.,  $NH_4^+$ ) and combinations of ions ( $Ca^{2+}$  and  $SO_4^{2-}$ ) were not included in the ECOS-Runsalt software. Thus, some limitations of the ECOS-Runsalt software were revealed. However, the ECOS-Runsalt software is very user friendly, provides fast results on  $RH_{eq}$ , and creates a reasonable overview of the present phases. Finally, having the possibility to determine the  $RH_{eq}$ , including the metastable contribution in salt mixtures, may be of value for obtaining new theoretical insights.

## Acknowledgements

Clifford Price is acknowledged for providing access to the executable ECOS file, and Michael Steiger is acknowledged for constructive comments on the manuscript.

## Funding

This project was financially supported by the Aage and Johanne Louis-Hansen Foundation.

## Competing interests

Not applicable

## References

- [1] Arnold A., Zehnder K. (1991), Monitoring wall paintings affected by soluble salts, in The conservation of wall paintings, S. Cather (eds.), The Getty Conservation Institute. pp. 103-135.
- [2] Sawdy A, Heritage A (2007), Evaluating the influence of mixture composition on the kinetics of salt damage in wall paintings using time lapse video imaging with direct data annotation. Environmental Geology volume 52. Pp. 303-315.
- [3] Laue S., Schaab C., Drese D., Krauthäuser, Helfmeier G., Vogt J. (2020), Long-Term investigations and monitoring of the salt loaded Crypt of St. Maria im Kapitol, Cologne. In: Siegesmund, S & Middendorf, B. (Eds.): Monument Future: Decay and conservation of stone. – Proceedings of the 14<sup>th</sup> International Congress on the deterioration and conservation of Stone – Volume I and volume II. Mitteldeutscher Verlag 2020. Pp. 345-350.
- [4] Steiger M. (2005), Salts in porous materials: Thermodynamics of phase transitions, Modeling and preventive Conservation. Restoration of Buildings and Monuments. Bauinstandsetzen und Baudenkmalpflege. Vol. 11, No 6. Pp. 419-432.
- [5] Bøllingtoft P., Larsen P.K. (2002), The use of passive climate control to prevent salt decay in Danish churches. Mauersalze und Architekturoberflächen: Tagungsbeiträge - Hochschule für Bildende Künste Dresden, Germany, 01.-03. Februar 2002. (Eds.) Leitner H., Laue H. pp. 90-93.
- [6] Brajer IE & Larsen PK (2008), The salt reduction treatment on the wall paintings in Tirsted Church. In *Proceeding of the conference Salt Weathering on Buildings and Stone Sculpture, Copenhagen, Denmark, 22-24 October 2008*. Pp. 219-228.
- [7] Pel L, Sawdy A, Voronina V (2010), Physical principles and efficiency of salt extraction by poulticing. Journal of Cultural Heritage 11. pp. 59–67.
- [8] Rörig-Dalgaard, I. (2009), Desalination for preservation of murals by electromigration and regulated climate. Structural Studies, Repairs and Maintenance of Heritage Architecture XI, (ed.) Brebbia C.A., Tallinn, Estonia, 2009. 71-82.
- [9] Greenspan L., Humidity Fixed Points of Binary Saturated Aqueous Solutions. Journal of research of the National Bureau of Standards – Physics and Chemistry, [81A], [1977], 89-96.

- [10] Linnow, K. Steiger, M. Determination of equilibrium humidities using temperature- and humidity-controlled X-ray diffraction (RH-XRD). *Anal. Chim. Acta.*, **2007**, 583, 197-201.
- [11] Tang, I.N. Munkelwitz, H.R. Aerosol Phase Transformation and Growth in the Atmosphere, *J. Appl. Meteorol.* **1994**, 33, 791-796.
- [12] Ge, Z. Wexler, A.S. Johnston, M.V. Deliquescence Behavior of Multicomponent Aerosols. *J. Phys. Chem* **1998**, 102, 173-180.
- [13] Steiger, M. Salts in Porous Materials, Thermodynamics of Phase Transitions, Modeling and Preventive Conservation. *Bauinstandsetzen und Baudenkmalpflege* **2005**, 11(6), 419-432.
- [14] Steiger, M. Asmussen, S. Crystallization of sodium sulfate phases in porous materials: The phase diagram  $\text{Na}_2\text{SO}_4\text{-H}_2\text{O}$  and the generation of stress. *Geochim. Cosmochim. Acta* **2008**, 72, 4291-4306.
- [15] S.L. Clegg, P. Brimblecombe, Z. Liang, C.K. Chan (1997), Thermodynamic Properties of Aqueous Aerosols to High Supersaturation: II-A Model of the System  $\text{Na}^+ - \text{Cl}^- - \text{NO}_3^- - \text{SO}_4^{2-}$ ,  $\text{H}_2\text{O}$  at 298.15 K, *Aerosol Science and Technology*, 27:3, 345-366.
- [16] Lindström N, Heitmann N., Linnow K., Steiger M. (2015), Crystallization behavior of  $\text{NaNO}_3\text{-Na}_2\text{SO}_4$  salt mixtures in sandstone and comparison to single salt behavior. *Applied Geochemistry* 63. Pp. 116-132.
- [17] De Clercq H (2008), The effect of other salts on the crystallization damage to stone caused by sodium sulphate. In *Proceeding of the conference Salt Weathering on Buildings and Stone Sculpture, Copenhagen, Denmark, 22-24 October 2008*. Pp. 307-316.
- [18] Bionda, D., 2005. RUNSALT - A graphical user interface to the ECOS thermodynamic model for the prediction of the behaviour of salt mixtures under changing climate conditions. <http://science.sdf-eu.org/runsalt/>
- [19] Price, C. A. (Ed.), 2000. An expert chemical model for determining the environmental conditions needed to prevent salt damage in porous materials. European Commission Research Report No 11, (Protection and Conservation of European Cultural Heritage). Archetype Publications, London. <http://science.sdf-eu.org/runsalt/>
- [20] Rörig-Dalgaard, I. (2012), Determination of the deliquescence point in salt mixtures by utilizing the dynamic vapour sorption method. The 3<sup>rd</sup> International Workshop on Crystallization in Porous Media. (ed.) Teresa Diaz, Troja, Portugal, 2012. 37-38.
- [21] Rörig-Dalgaard, I.; Svensson S. (2016), High accuracy calibration of a dynamic vapor sorption instrument and determination of the equilibrium relative humidity of single salts. Citation: Review of Scientific Instruments 87 (5), 054101 (2016); doi: 10.1063/1.4949513
- [22] Rörig-Dalgaard, I. (2014), Determination of the deliquesce point in salt mixtures and in in-situ multicomponent salts with DVS equipment. "Salt Weathering on Buildings and Stone Sculptures, SWBSS 2014", Brussels, Belgium, 14-16 October 2014. 223-236.
- [23] Steiger M, Kiekbusch J, Nicolai A (2008). An improved model incorporating Pitzer's equations for calculation of thermodynamic properties of pore solutions implemented into an efficient program code. *Construction and Building Materials* 22 (2008) 1841–1850.
- [24] Koloutsou-Vakakis, S. Rood, M.J (1994). The  $(\text{NH}_4)_2\text{SO}_4\text{-Na}_2\text{SO}_4\text{-H}_2\text{O}$  system: comparison of deliquescence humidities measured in the field and estimated from laboratory measurements and thermodynamic modelling. *Tellus, 46B*, 1-15.
- [25] Rijck, G.D. Schrevens, E (1998). Elemental bioavailability in nutrient solutions in relation to precipitation reactions. *J. Plant Nutr.*, 21(10), 2103-2113.
- [26] Heng J. Y.Y. & Williams D.R. (2011), Vapour Sorption and Surface Analysis, chapter 8 in Solid State Characterization of Pharmaceuticals, first edition. Edited by Storey R.A. and Ymén I. Blackwell Publishing Ltd. Published 2011 by Blackwell Publishing Ltd. ISBN: 978-405-13494-1.
- [27] R. C. Weast (1983), "CRC Handbook of Chemistry and Physics 1983-1984," 64th Edition, CRC, Boca Raton.
- [28] Bläuer Böhm, C. (1996). Praktische Hinweise zur Vorgehensweise bei der Untersuchung und Beurteilung von salzbelasteten Baudenkälern. Salzschäden an Wandmalereien. Beiträge der Fortbildungsveranstaltung der Restaurierungswerkstätte 28./29. November 1988. Arbeithefte des Bayerischen Landesamtes für Denkmalpflege, Heft 78, Seiten 39-52.

- [29] Rörig-Dalgaard, I 2014, Transition at the deliquesce point in single salts. in *Proceedings of the 4th international workshop on crystallization in porous media*. 4th international workshop on crystallization in porous media, Amsterdam, Netherlands, 11/06/2014.

## Figures



**Figure 1**

Absorption of water molecules on 25 mg of NaCl(s) followed by vapor condensation in an aluminium pan ( $d = 6 \text{ mm}$ ); a 453 % weight gain is observed. A weight gain of only 278 % is needed to ensure the complete dissolution of NaCl.

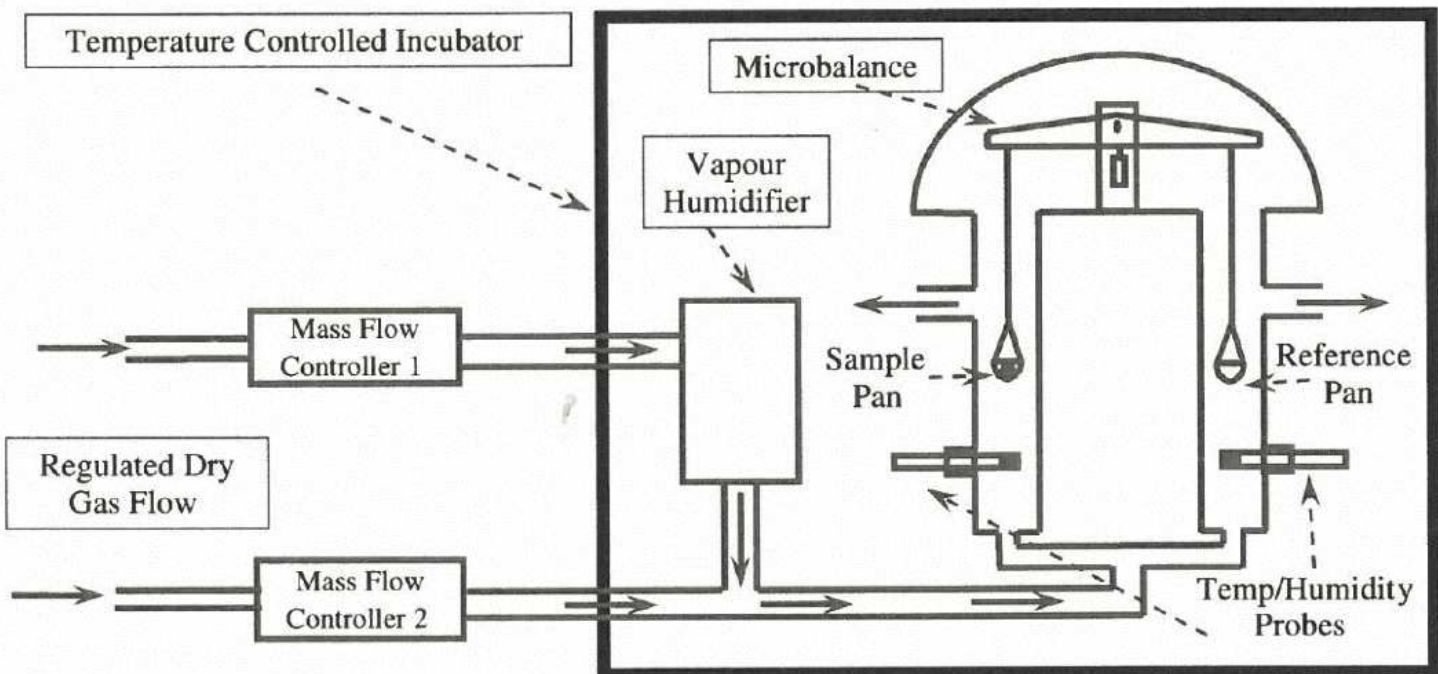


**Figure 2**

Schematic of the DVS instrument. Solid arrows show the direction of carrier gas flow. Reproduced with permission from [26].

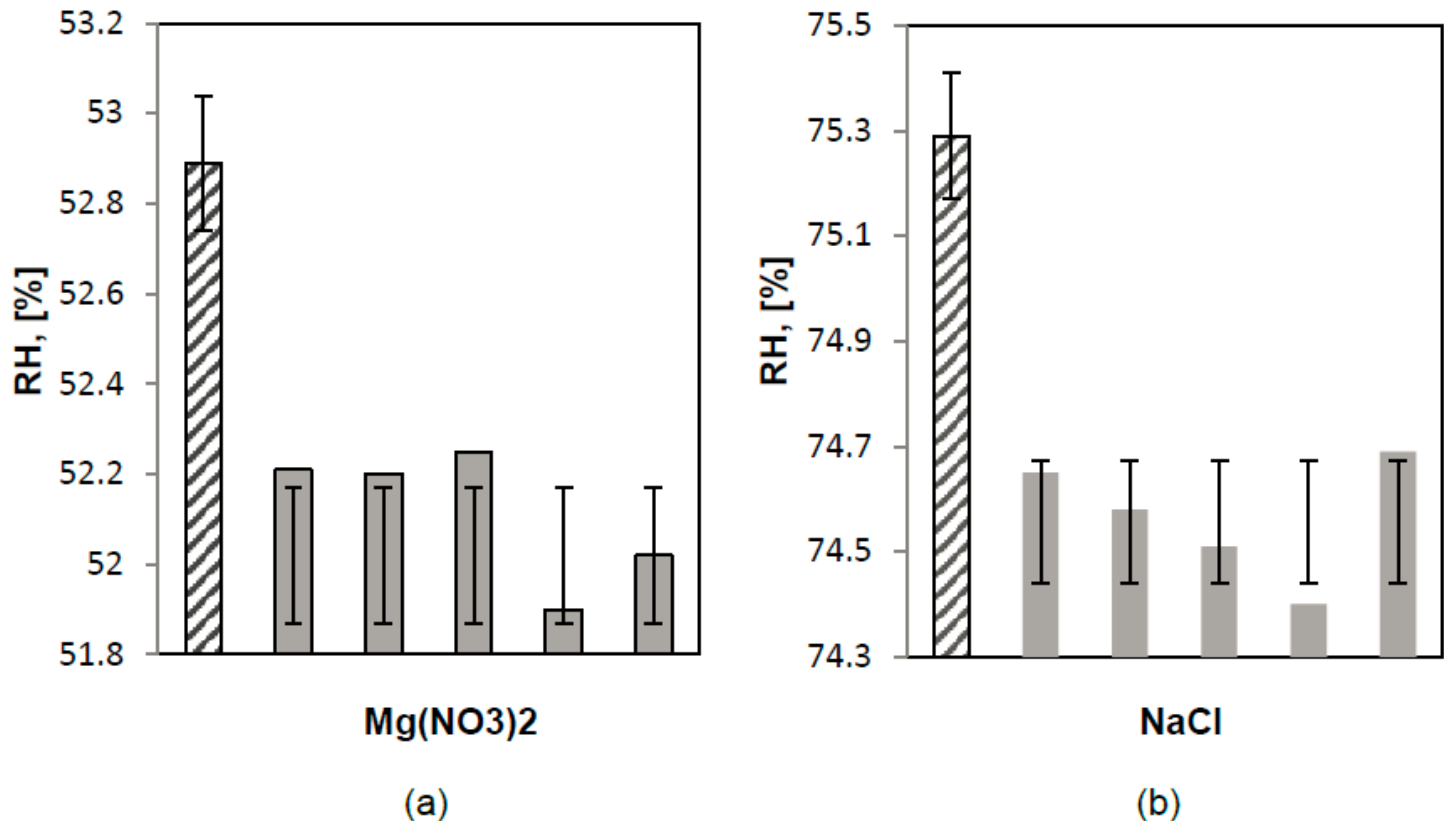


**Figure 3**

Reference RHeq from the literature [2] (shaded bars) together with experimentally obtained RHeq, DVS (solid bars), shown for a) Mg(NO<sub>3</sub>)<sub>2</sub> and (b) NaCl salts.

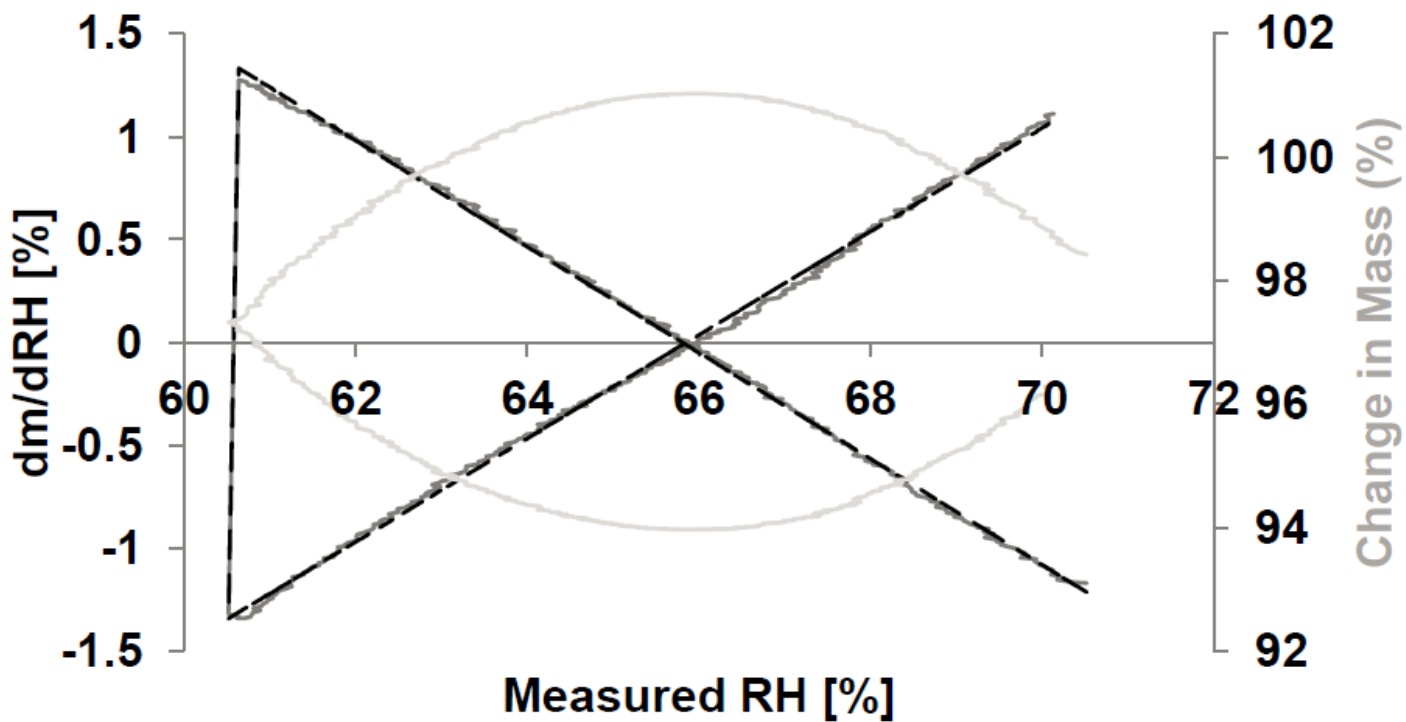


**Figure 4**

Example of the measurement results enabling the determination of the RHeq of the salt mixture NaCl-Na<sub>2</sub>SO<sub>4</sub>-NaNO<sub>3</sub> at 25.0°C. ☐ (dark grey solid line) Measured dm/d RH with the dew point analyser within the sample chamber, ☐ (black dotted line) fitted dm/dRH, ☐ (bright grey solid line) change in mass in %.

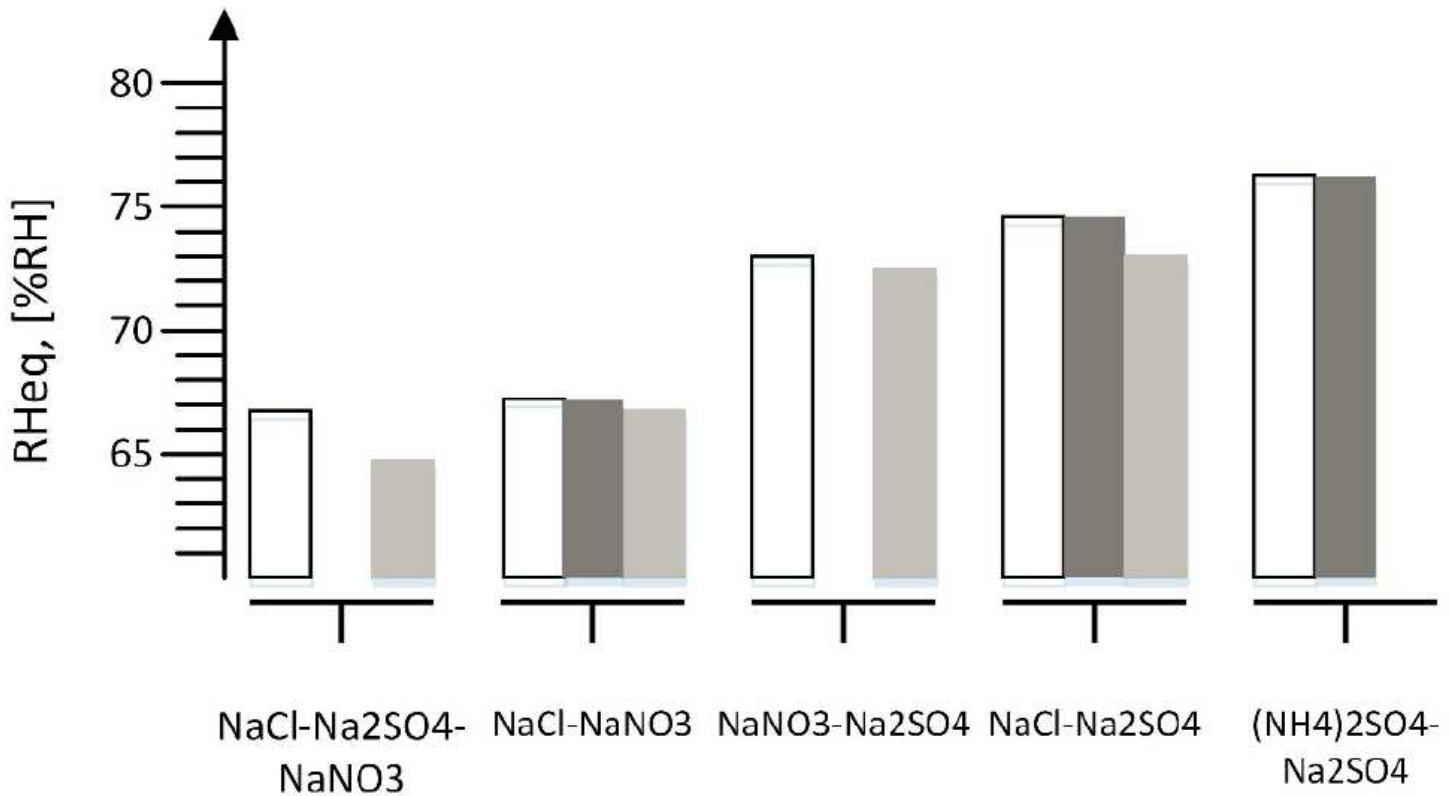


**Figure 5**

RHeq of salt mixtures as obtained by different determination methods. white- RHeq (re-cal, DVS) from Table 3 dark-gray- Experimental data from the literature and light-gray- calculated results from the thermodynamically based ECOS-Runsalt model.

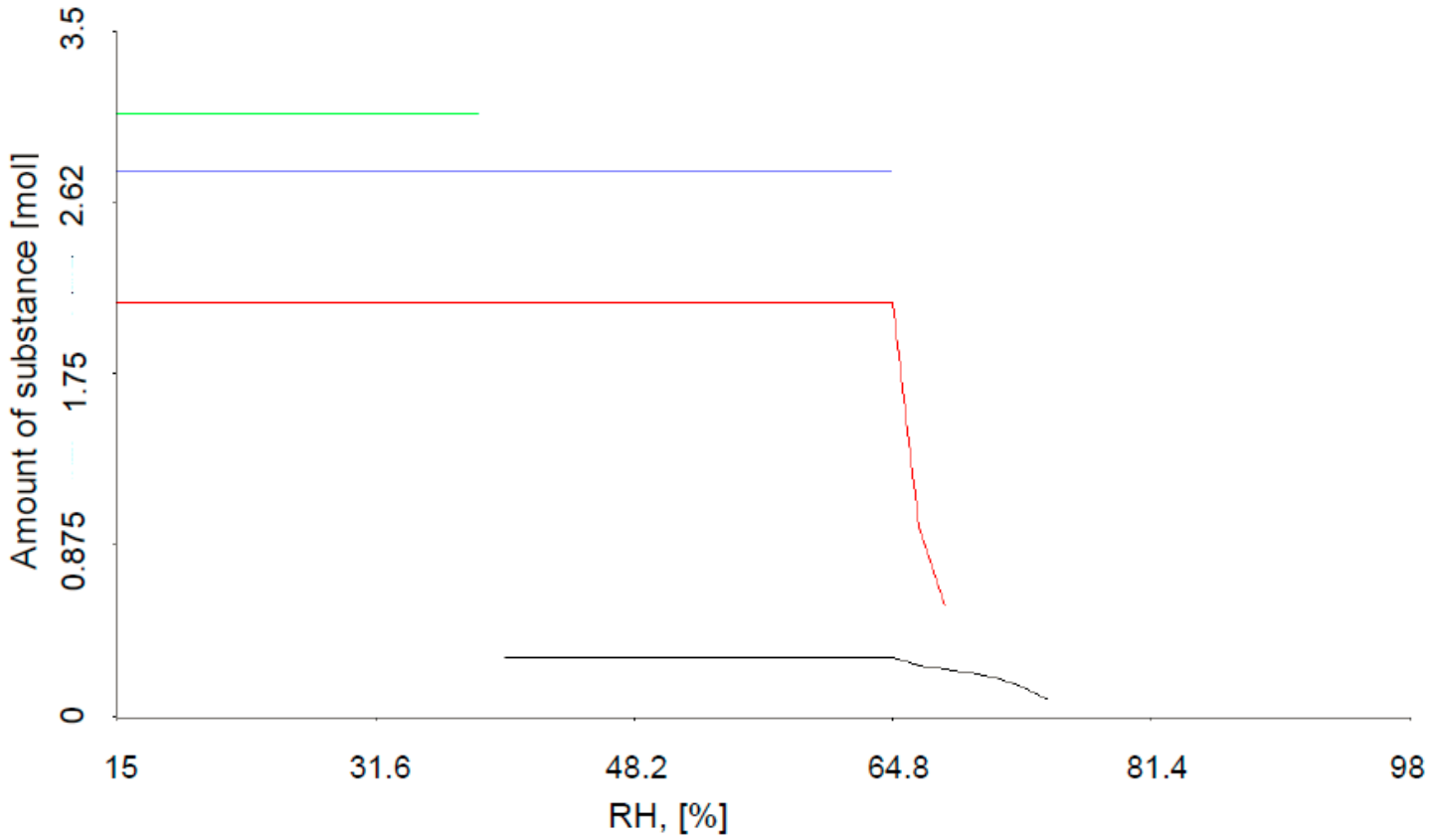
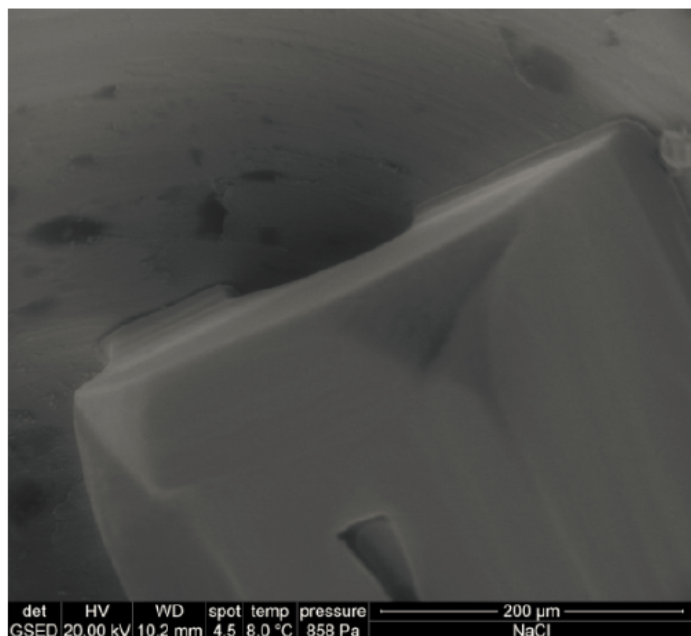
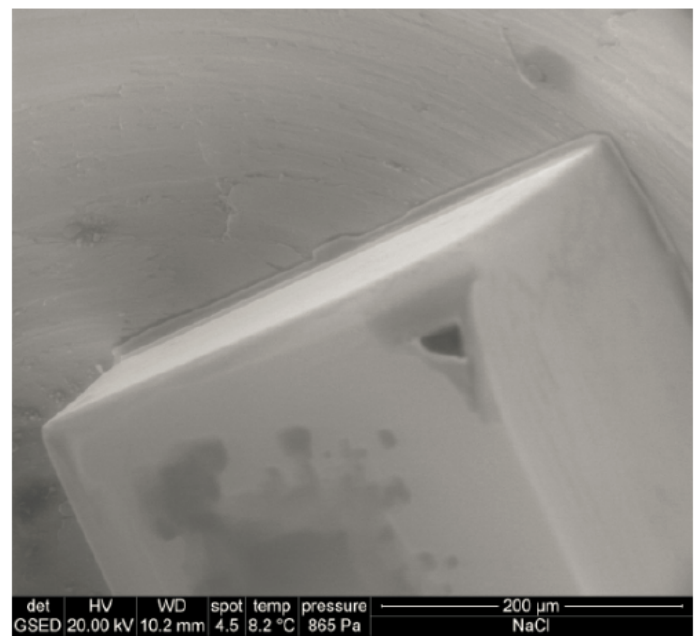


**Figure 6**

ECOS-Runsalt output diagram for the salt mixture NaCl-Na<sub>2</sub>SO<sub>4</sub>-NaNO<sub>3</sub> with the number of moles being 3.4, 0.7, 0.3 and 2.1 for sodium, chloride, sulfate and nitrate, respectively, at 25°C. The RHeq (ECOS-Runsalt) was calculated to be 64.8 %. Black indicates the content of darapskite (NaNO<sub>3</sub>Na<sub>2</sub>SO<sub>4</sub>·H<sub>2</sub>O), red indicates nitratine (NaNO<sub>3</sub>), blue indicates halite (NaCl) and green indicates thenardite (Na<sub>2</sub>SO<sub>4</sub>).



(a)



(b)

## **Figure 7**

Visualization of the kinetic influence ( $\Delta RH$ ) on a salt (NaCl) phase transition studied by the application of a cooling stage in an ESEM: a) reference equilibrium conditions and b) influence of a change of 0.1 % RH for 19 hours [29].